Proceedings of the
Annual Stability Conference
Structural Stability Research Council
Louisville, Kentucky, April 2-4, 2025

Sensitivity of open-web steel joist stability to material and geometric property variability

Kubilay Cicek[1],Thomas Sputo[2], Hannah B. Blum[3]

Abstract

Open-web steel joists are commonly used as roof framing members. These joists are composed of angle, U-channel, and rod sections welded together into trusses to resist applied loads as an indeterminate system. The angle and channel sections may be either hot-rolled or cold-formed sections, depending upon manufacturer preferences. Potential joist failure modes include yielding in the tension chord and webs, or buckling of the compression chord and webs. The resulting failure mode depends on the specific joint details in addition to uncertainty in the parameters affecting strength. A structural reliability study of open-web steel joists was conducted which considered variability of material properties (yield and ultimate strength), geometric properties of the cross sections, and weld length, for joists comprising both hot-rolled and cold-formed sections. The variability of these properties was based upon data collected from joist manufacturers.

The joists in this study were proportioned to be controlled by limit states of (1) tension chord yielding, (2) tension web yielding, and (3) compression web bucking (both geometric or local). The joists were modeled using shell elements in ABAQUS to validate the behavior of beam-element models, which were subsequently used in the study. Appropriate joint restraint and chord bracing as provided by bridging or steel deck attachment was included. Multiple non-linear analyses were performed using statistical distributions of the variabilities, including appropriate notional loads to seed buckling. Results show that when compared against models using nominal properties, that material property variability has a greater influence on buckling resistance than geometric imperfections or weld length.

1. Introduction

Open web steel joists (OWSJ) are efficient systems with their lightweight features and adaptable designs while providing high load carrying capacity. They are widely used as a member in roof framing systems in construction and typically made from hot-rolled steel (HRS) or cold-formed steel (CFS) sections. Combinations of multiple members such as chords and webs create an indeterminate structure providing alternate load paths in the event of failure of a single member.

[1]PhD Student, University of Wisconsin-Madison, <cicek@wisc.edu>
[2]Technical Director, Steel Deck Institute, <tsputo50@gmail.com>
[3]Alain H. Peyrot Associate Professor, University of Wisconsin-Madison, <hannah.blum@wisc.edu>

While the internally indeterminate nature of joists can be beneficial to structural safety, the performance of thin members are highly dependent on several key factors, including material properties, geometric characteristics, and the length of welded connections. These factors can influence the stability and reliability of the designed joist systems and require a further study to indicate the importance levels of each individual factor.

A sensitivity study is one of the methods that can quantify the influence of a selected parameter on the performance of a given system. This study focuses on two different joist geometry comprised of HRS or CFS sections which were designed by Steel Joist Institute (SJI) member manufacturers. The sensitivity of their behavior to variability in material properties, geometric imperfections, and weld lengths is explored. SJI member manufacturer collected data was used as the sensitivity analysis inputs. Three critical failure modes were considered in this analysis including both tension and compression failures to explore the sensitivity of parameters in broader perspective.

For this purpose, advanced finite element (FE) modeling was employed with 3D shell elements using ABAQUS(Abaqus, 2016) software. Detailed 3D shell element models were used in second order nonlinear analyses with the incorporated material and geometric nonlinearities with realistic welded connections and support conditions. After the validation of these shell element FE models, more efficient yet highly accurate beam element FE models were created using ABAQUS(Abaqus, 2016), and those were validated with the previously created shell element models. These beam element models offered computational efficiency while maintaining high accuracy with the modified features of the joist models.

A comprehensive sensitivity analysis was conducted using statistical distributions of the collected data. Six primary models representing combinations of joist types and failure modes were used to perform the simulations and the results were evaluated according to these different designs. Sensitivity results show that the material behavior and strength has the dominant influence on both yielding and buckling failures of joists. Cross-sectional imperfections also showed a significant effect on the joist strength but but to a lesser degree as the material properties. Weld length however was found to have negligible to no impact on the stability of the system within the collected data range. These findings provide critical observations on the factors affecting the stability of the open-web steel joists and highlight the importance of the selected parameters in the design and manufacturing phases.

2. Selected Joist Designs and Failure Modes

The SJI member manufacturers provided the joist designs for this study. Two main joist designs were considered, both with a 50 ft span and 30-inch depth. The generic designs for these joists are presented in Figs. 1 and 2, showing Joist I (hot-rolled steel members) and Joist II (cold-formed steel members), respectively. By keeping the same initial layouts, specific members of these joists were redesigned to achieve the selected failure mode under the maximum loads. The maximum loads were updated according to the selected failure modes, which are:

- Bottom chord tension yielding,
- First web tension yielding (W2 web - first tension web),

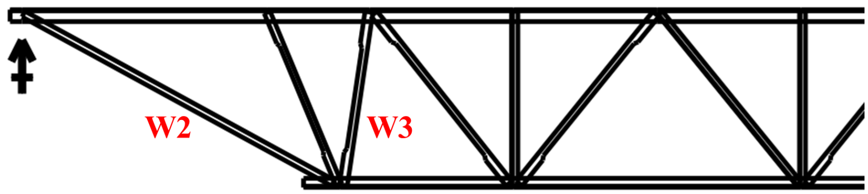

Figure 1: Joist with HRS sections (Joist I)

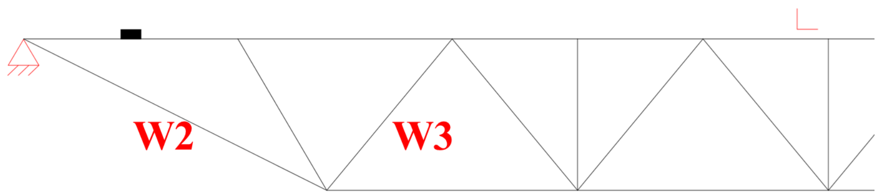

Figure 2: Joist with CFS sections (Joist II)

- First compression web buckling (W3 web - first compression web).

Joist design assumptions and the impacts of these assumptions were discussed in a previous study (Cicek, Sputo, and Blum, 2024)). Detailed 3D shell FE models were generated for six different joists models (two joist types with three different failure modes each) to capture the actual failure modes and to compare the model performance with design predictions. In this study, beam FE models were created in ABAQUS for sensitivity analysis, and shell FE models were used to validate these beam FE models.

3. Finite Element Models

ABAQUS software was used to generate FE models of designed joists. Material and geometric nonlinearities were incorporated through second order nonlinear analyses to determine the actual capacity of the designed joists. Welded connections, loading, end, and lateral supports were modeled following the guidance provided by the SJI and SDI member companies' research teams. Fig. 3 shows the section types used in the selected joist designs.

Single HRS angle sections were used in webs (crimped at 6 inches on both ends to fit between the top and bottom chords) and as double-angle sections on chords in Joist I. Additionally, first web members in Joist I were designed as rod sections whereas CFS channel sections were used for all web members in Joist II, with CFS double-angle sections for the chords.

Both shell and beam element FE models employed consistent approaches for sectional properties, material models, loads, and supports. Loads were calculated for uniformly distributed loads in the design process and applied as distributed gravity loads to the top chord double angle members. The designed system was modeled with simple beam end conditions, a pinned connection at one end and a roller connection at the other. End plates were modeled separately and connected to the top chord members, and the support conditions were assigned to the end plates. Lateral supports were modeled similarly to real-world joist-deck systems, with 12-inch spacing (alternating between

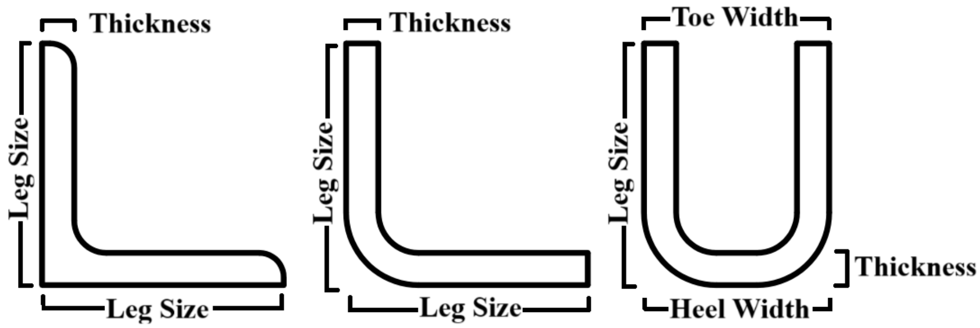

Figure 3: Left: HRS angle, Middle: CFS Angle, Right: CFS Channel sections

chord double-angle sections) for the top chord lateral supports and lateral supports for the bottom chord angles at each panel point. The top chord bracing spacing simulated steel roof deck fastened at 12 inches on center.

Different material models were created for HRS and CFS members, where both were applied in shell and beam FE models. The material properties for HRS sections were based on Yun et al. (2017) while CFS section material models were taken from Gardner et al. (2018). Both joist designs assumed a nominal material yield strength of 345 MPa (50 ksi) with an elasticity modulus of 200 GPa (29,000 ksi) (AISC 360-16, 2016) for HRS sections and 203.4 GPa (29,500 ksi) (American Iron and Steel Institute, 2020) for CFS sections. Fig. 4 shows the material models for both HRS and CFS material models.

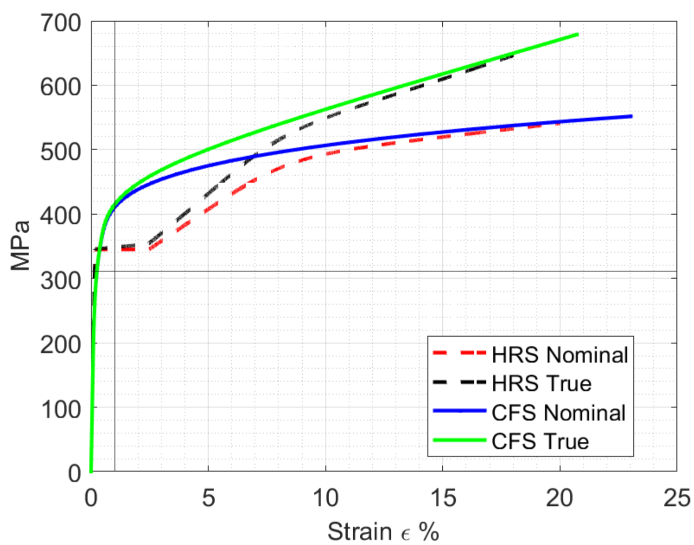

Figure 4: Material models for HRS and CFS sections

An important feature of the FE modeling is including the initial imperfections in regions where buckling is expected. For the first compression web (W3 web) failure, where buckling is the expected failure mode, initial imperfections were accounted for by applying notional loads. These notional loads N were calculated by Eq. 1:

$$N = 0.002 F_y A \tag{1}$$

where F_y is the yield stress of W3 web material, and A is the cross-sectional area of the W3 web. Values for F_y and A were updated at each simulation based on the assigned inputs of the W3 web.

3.1 Shell Finite Element Models

The sections were modeled and assembled according to the given designs, and features such as crimped angle section webs and welds, were also modeled. All sections were modeled with S4R shell elements except for the round rod sections and the filler elements between the chord angles, which were modeled with C3D8R solid elements. Further details on shell models were provided in the previous paper (Cicek, Sputo, and Blum, 2024).

Welded connections were modeled by using tie connections along the edges of web members to simulate weld lines. For filler to chord connections and rod to chord connections, double bevel welds were modeled with an additional weld element. The interaction between the weld elements and the welded components was modeled using surface-to-surface connections. Figs. 5a and 5b show the weld lines and double-bevel weld elements with connection surface for welded connections.

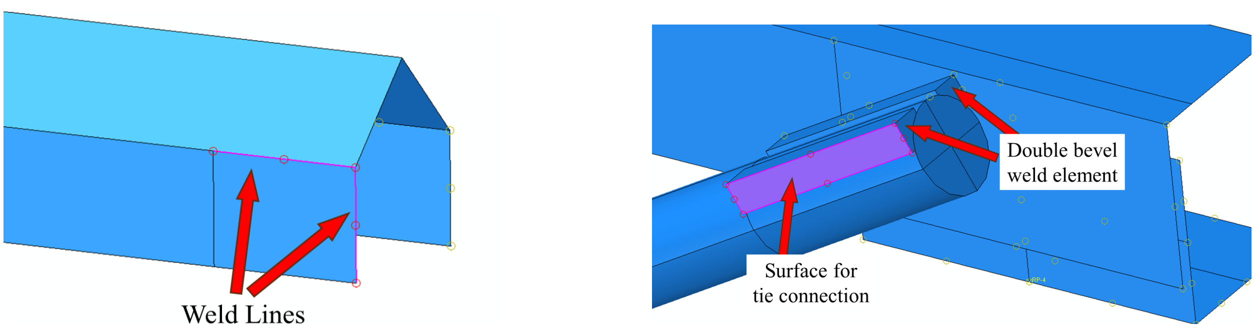

(a) Weld line tie connections for open section welds

(b) Surface to surface tie connections shown for a rod end connection

Figure 5: Connection types and applications (Cicek, Sputo, and Blum, 2024)

Joist I has HRS angle sections for web members, which are crimped on both ends to fit in between double angles chord sections. The crimpings starts from 6 inches on both ends of the angle webs (Fig. 6). These crimpings affect the stiffness of welded connection by changing both the total welded area and the moment of inertia of the web members. To capture this effect, crimping was also modeled in ABAQUS shell FE models.

Shell element models were verified by comparing the ultimate load and vertical deflection results with the given design results for first-order linear models. The comparison results are provided in Table 1.

3.2 Shell FE Models for Moment-Rotation Stiffness

Shell element models were also modified and used to create a portion of the joist to calculate the stiffness of the welded connection for later use in beam element FE models. These stiffness

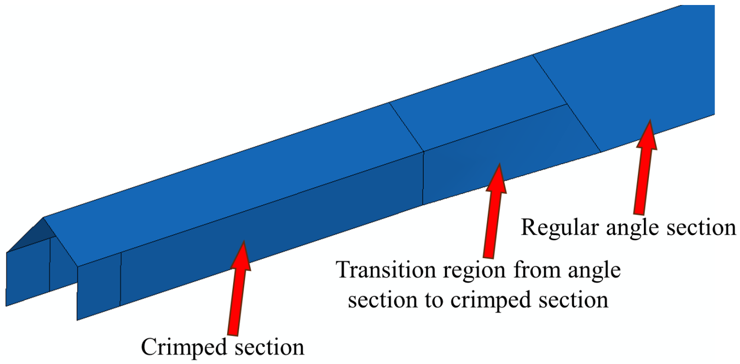

Figure 6: HRS angle web crimped at 6 inches at the ends (Cicek, Sputo, and Blum, 2024)

Table 1: Vertical deflection at mid-span comparison between manufacturer model predictions and shell FEM results under design loads

	Joist I			**Joist II**		
Failure Mode	SJI-model (in)	Shell FEM (in)	Diff (%)	SJI-model (in)	Shell FEM (in)	Diff (%)
BC	1.67	1.685	0.90	1.60	1.636	2.22
FW	1.67	1.642	1.67	1.60	1.600	0
W3	1.67	1.640	1.79	1.60	1.631	1.94

Modes: BC: bottom chord failure, FW: first web failure, W3: first web buckling failure

values were used to define springs located at the end web connections to increase the accuracy of the joist models. Three different shell model analyses with possible minimum, maximum, and mean weld lengths, based on collected weld length data, were completed. After the minimum and maximum boundaries with a middle point (mean value result) were determined by shell models results, linear interpolation was used to estimate the web end connection stiffness by changing weld length at each simulation. Fig. 7 shows the modified shell element models for calculation of moment-rotation values of CFS sections, and the analysis result of the corresponding model.

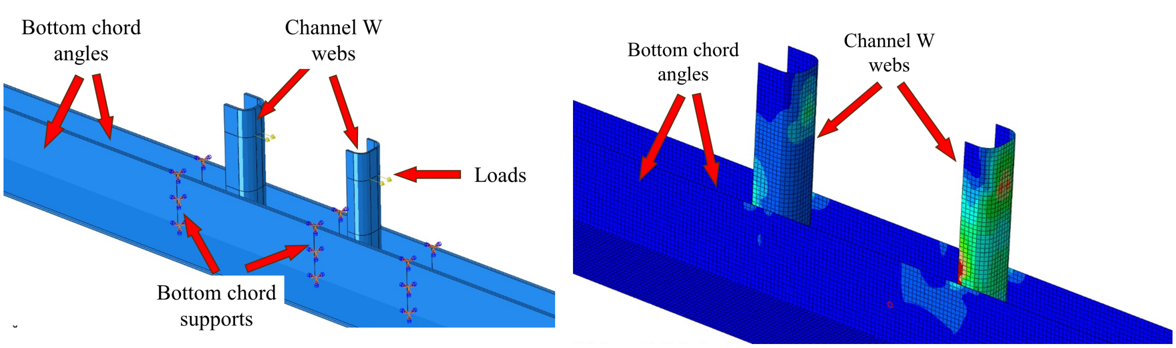

(a) Loads and modified members

(b) Results for moment-rotation analysis

Figure 7: Modified shell element models for web rotational stiffness calculations (Joist II)

3.3 Beam Finite Element Models

Although the beam models might have a limited ability to represent geometrical details and to obtain possible local buckling failures, with suitable modifications the generated models are capable of capturing the joist behavior with high accuracy while providing a significant computational time savings. The given joist designs were modeled by using B33 beam elements in ABAQUS, and second order nonlinear analyses were completed to represent both geometric and material nonlinearity.

One of the important upgrade to beam element models was use of spring end connections on web-to-chord connections. Equivalent spring connections for each web group were assigned to web end connections with the specified stiffness values that were obtained by modified shell element models as specified in Section 3.1. The spring values were calculated based on the nominal weld length values to align with the nominal system inputs. Incorporating weld length effects by using identical stiffness springs at web ends improved the accuracy of beam element models and resulted in different LPF values compared to models with fixed or pinned web ends.

A major modification to beam element models was including reduced yield strength of the W3 web materials to represent the impact of local buckling. While the shell models clearly showed W3 web buckling failure, beam element models showed no buckling and resulted with around 12-15% higher load capacity than shell element models. Several studies (Trahair and Hancock, 2004, Kucukler et. al., 2014, Zhang et. al., 2015, Rasmussen et. al., 2016) suggest that reducing the capacity of members in beam element models can increase the accuracy between the shell and beam element models by representing the impact of local buckling. In this study, it was found that reducing the yield strength of only W3 web members rather than changing the elasticity of the W3 web members, resulted in high accuracy between the shell and beam models and an agreement in failure modes. For Joist I the yield strength was reduced by 0.8, as suggested in Section C2.3(a) of Chapter C in AISC 360-22 (2022), and for Joist II the yield strength was reduced by 0.9.

After the modifications were completed, all beam element models were validated by comparing with shell element model results. Table 2 shows maximum load proportionality factor (LPF) value comparison and Fig. 8 shows the load - deflection curve comparisons of beam and shell element analyses for each failure mode and for each joist type. Comparisons show a good match between the models. Another outcome of these results is that despite assigning every input with their nominal value, the capacities are higher than the SJI design calculated capacities due to the included material nonlinearity and post-yield strength and higher overall joist stiffness with the included semi-rigid web end connections. The difference in capacities are even higher for the CFS joists and this also proves that the material model has a high impact in the calculated capacity as can be seen in material models Fig. 4.

4. Collected Data, Distribution Parameters and Sensitivity Study

4.1 Collected Data and Fitted Distributions

The data used in this study were collected by SJI member companies as part of a broader study to evaluate the reliability of steel joists. The input parameters of material strength, cross-sectional geometry, and weld lengths, were collected from their manufacturing facilities. Then the distribution fitting process was performed on the collected data by normalizing the measured values

Table 2: Maximum Load Factor (LPF) comparison between shell element FE and beam element FE models (with 10 inches of deflection limit applied)

	Joist I			Joist II		
Failure Mode	Shell Element	Beam Element	Diff (%)	Shell Element	Beam Element	Diff (%)
BC	1.096	1.109	1.186	1.414	1.416	0.141
FW	1.100	1.106	0.545	1.579	1.560	1.203
W3	1.290	1.323	2.558	1.364	1.313	3.739

Modes: BC: bottom chord failure, FW: first web failure, W3: first web buckling failure

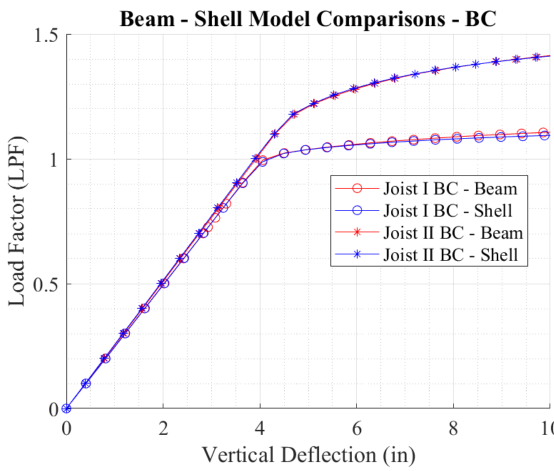

(a) BC yielding failure mode models

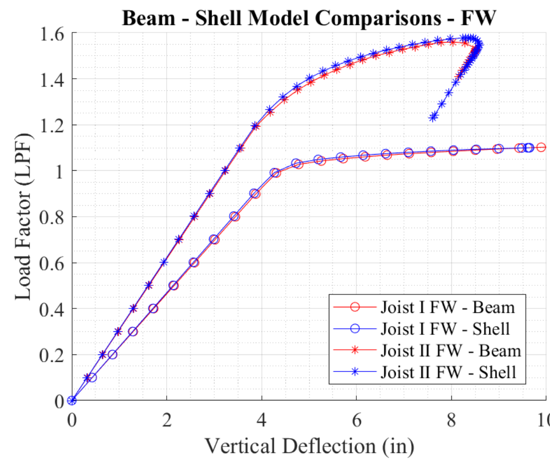

(b) FW yielding failure mode models

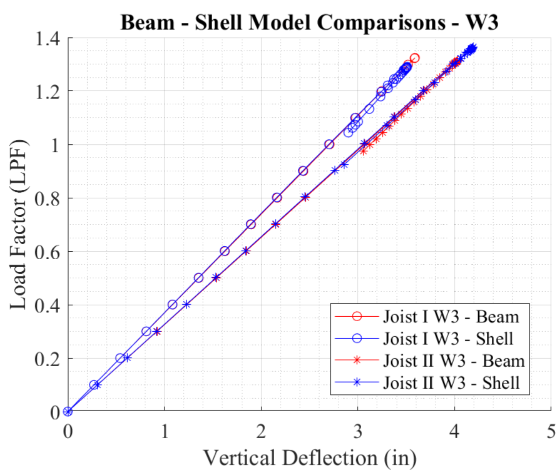

(c) W3 web buckling mode models

Figure 8: Load - Deflection curve comparison for beam and shell element FE models

with respect to their corresponding nominal values. This normalization provides a consistency in generating random variables for multiple analyses. The best fit distributions were calculated and the distribution types and calculated mean and standard deviation values are provided in Figs. 9 to 13 and in Table 3.

For material data, tensile stress tests coming from 345 MPa (50 ksi) materials were collected and the collected data were normalized with the nominal value of 345 MPa (50 ksi) as the selected material. Whereas the cross-sectional measurements and weld length measurement were collected from variety of joists and joist members as can be seen in Fig. 3. Therefore, the normalization was completed with the variety of nominal values determined from each data collected member.

The weld length data was collected from the first six webs of both sides of the joists by the SJI member companies. Based on this data, the distribution fitting process was completed. It was observed that W2 members and vertical members exhibited distinct standard deviations due to their angles relative to the chord members. Therefore, three groups for weld length data were formed: W2 webs, vertical webs and W webs. Separate distribution fitting processes were applied to each group. The spring stiffness values of each web member in the joists were assigned based on the group to which they belong, with the corresponding distribution parameters provided in Table 3.

Table 3: Fitted distribution types and calculated parameters of collected data (relative to nominal)

Collected Data	Distribution Type	Mean	Standard Deviation	Number of Data
HRS Yield Stress	Burr Dist.	1.098	0.173	336
CFS Yield Stress	Frechet Dist.	1.237	0.124	265
HRS Leg Size	Lognormal Dist.	1.001	0.011	377
HRS Thickness	Stable Dist.	1.005	-	740
CFS Leg Size	Burr Dist.	1.015	0.142	365
CFS Thickness	Frechet Dist.	0.980	0.033	717
CFS Ch. Heel Width	Burr Dist.	0.985	0.141	89
CFS Ch. Toe Width	Frechet Dist.	1.020	0.042	88
W Webs Weld Length	Frechet Dist.	1.427	0.402	4163
W2 Webs Weld Length	Frechet Dist.	1.712	0.666	1380
Vert. Webs Weld Length	Frechet Dist.	1.900	0.629	2725

4.2 Random Number Generation

For the random number generation, the distributions and parameters provided in Table 3 were used with Latin Hypercube Sampling (LHS). The LHS method has been shown to reduce the necessary number of samples, hence the number of analyses, while still acquiring a high performance (Olsson and Sandberg, 2002). The LHS method was used with predefined truncation limits. Truncated distributions are particularly important for accurate data inputs and reducing the computational time, as the truncated distributions prevent the use of irrational values. Truncated values were selected based on professional judgment. Figs. 9 through 13 present the generated data distributions used in the sensitivity study based the collected data.

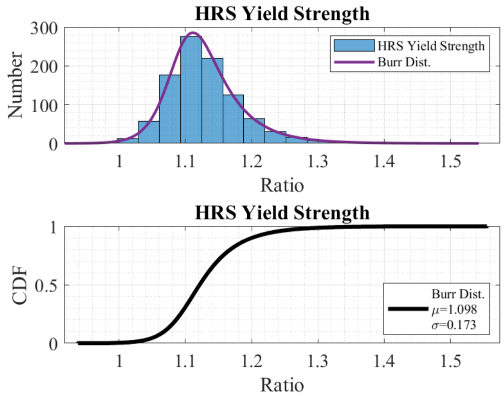

(a) HRS yield stress values

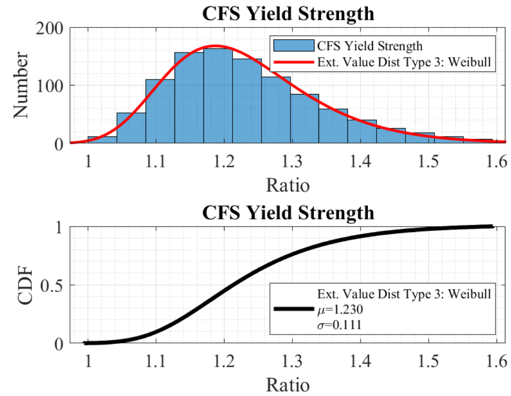

(b) CFS yield stress values

Figure 9: Histogram and statistical parameters of generated random yield stress values

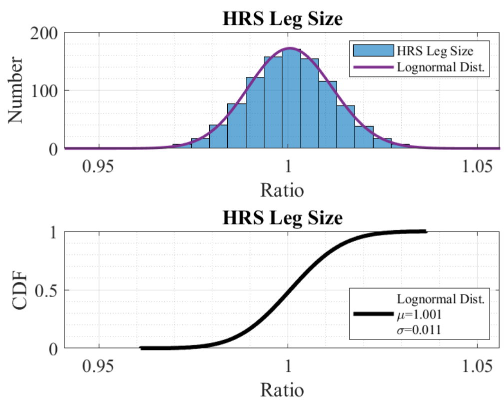

(a) HRS leg size values

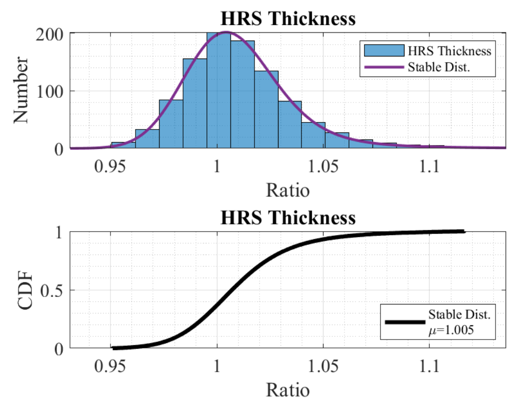

(b) HRS thickness values

Figure 10: Histogram and statistical parameters of generated random HRS cross-sectional values

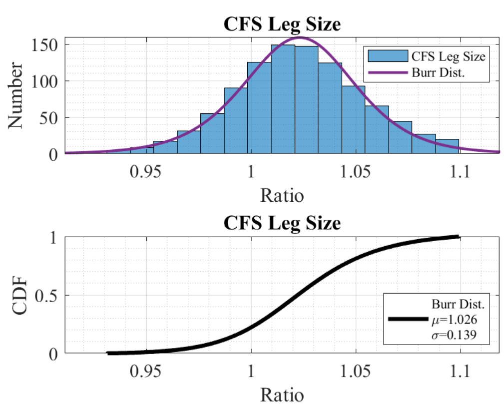

(a) CFS leg size values

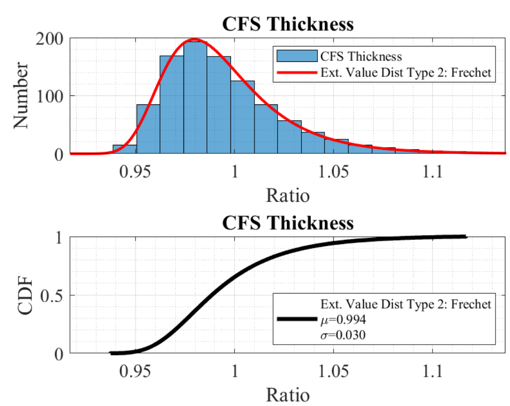

(b) CFS thickness values

Figure 11: Histogram and statistical parameters of generated random CFS cross-sectional values

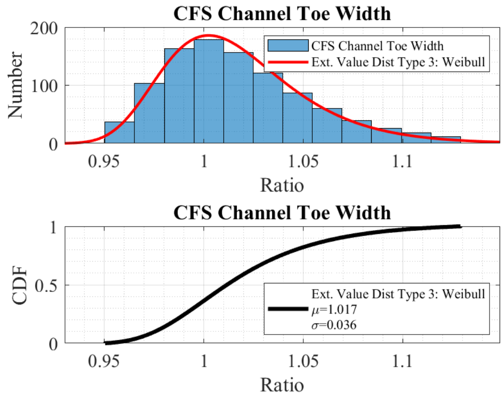

(a) CFS channel toe width values

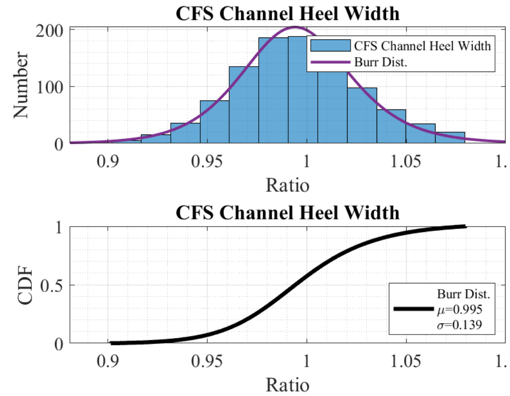

(b) CFS channel heel width values

Figure 12: Histogram and statistical parameters of generated random CFS cross-sectional width values

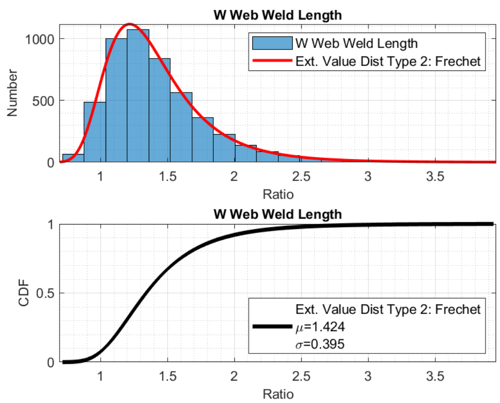

(a) W webs weld length values

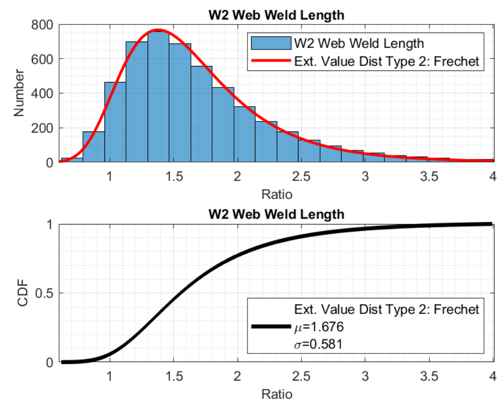

(b) W2 webs weld length values

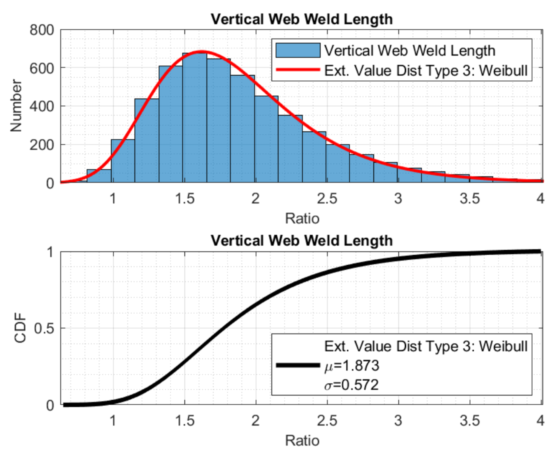

(c) Vertical webs weld length values

Figure 13: Histogram and statistical parameters of generated random weld lengths values

4.3 Sensitivity Analysis

Sensitivity analyses were conducted to evaluate the effect of the input variables previously mentioned on the performance of the nominal design joists. Sensitivity analyses were completed on six primary models including both Joist I, and Joist II, with three failure modes, to ensure a comprehensive assessment of different material and design characteristics. The study used nominal design joists rather than mean value designs to align with standard design practices.

In the sensitivity analysis process, one input parameter was systematically varied at a time while keeping all other parameters at their nominal values. Random samples for the selected parameter were generated based on the predefined statistical distribution which was detailed in Section 4.1. Using random samples from the collected data ensures a realistic representation of variability in the input parameter. Each simulation incorporated a random value from the input parameter into the finite element model, enabling the assessment of input parameter impacts on joist behavior.

For each of the six primary models, the sensitivity study was conducted for three failure modes, with sufficient simulations performed to capture the variability and sensitivity of the input parameters. The number of simulations was determined based on the stabilization of the mean Load Proportionality Factor (LPF) values, with the process terminating once a plateau was observed. Although the number of analysis was primarily determined by stabilization of mean value of LPF results after each analysis, it was aimed to have at least 1,000 analyses results to ensure the accuracy in distribution fitting. An output example for process is shown in Fig. 14 Additionally, to enhance the reliability of the outcomes, prematurely terminated analyses were discarded from distribution fitting process.

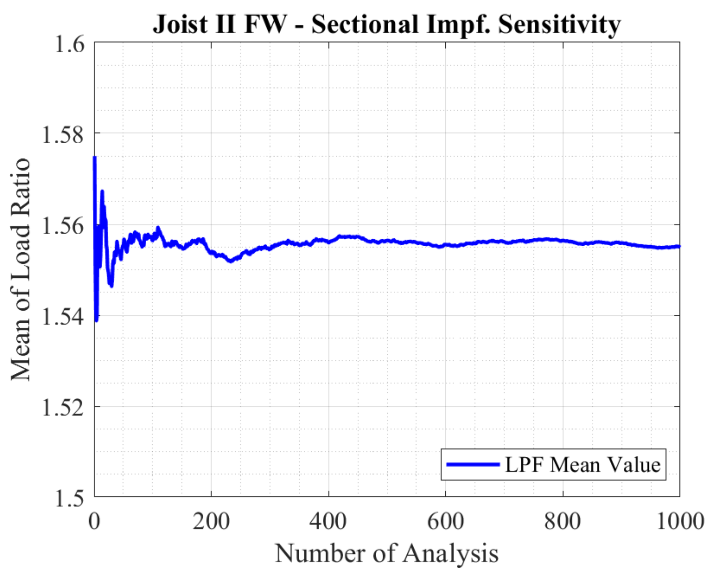

Figure 14: Mean LPF values after each analysis

5. Results

The sensitivity analysis was completed for material properties, cross-sectional imperfections, and weld lengths to reveal the influence of these parameters on the structural performance of both HRS and CFS joists. The process was completed by keeping all the inputs at their nominal value except the selected parameters with a randomly assigned value at each simulation.

5.1 Weld Length Sensitivity

Despite accounting for the effect of weld lengths in models, the sensitivity analysis showed that variations in weld length have negligible impact on the load capacity of joists. For all 1,000 analyses conducted for each model, the LPF values remained unchanged or insignificantly small changes were captured, as shown in Fig. 15 for Joist I BC failure mode as an example. This indicates that the given range of weld length variations within the collected data is not sufficient to influence the overall joist capacity significantly. Therefore, the weld length results were excluded from the results presented in this paper, as they do not contribute to the sensitivity findings for any of the six models.

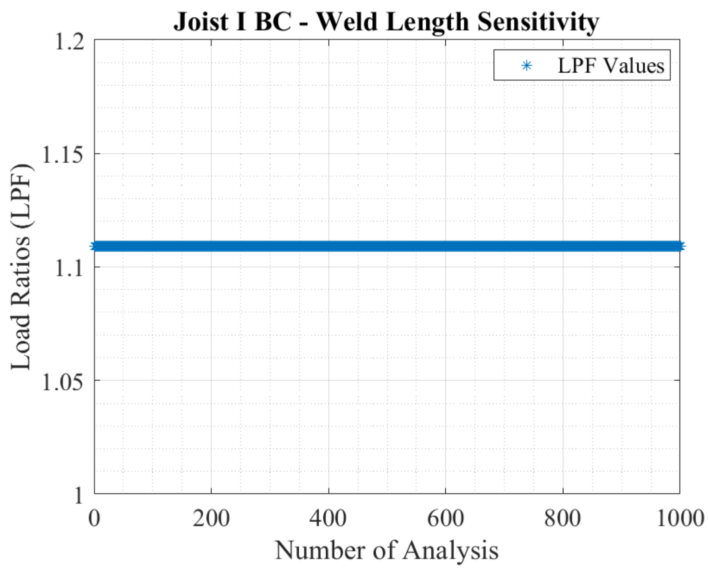

Figure 15: LPF values at each analysis

5.2 Cross-Sectional Imperfection Sensitivity

The mean LPF values calculated from the cross-sectional imperfection sensitivity analysis show no significant differences compared to the mean LPF values obtained from the beam element FE models with nominal system parameters. However, as Figs. 16 through 21 show that there is a significant spread in all failure modes due to variation in cross-sectional imperfections. The capacity can reduce between 5% to 15% from the calculated mean LPF values under certain conditions depending on the failure mode and joist design. This highlights the importance of quality controls of cross-section manufacturing processes.

5.3 Yield Strength Sensitivity

For both HRS and CFS joists, yield strength was found to be the most influential parameter, significantly affecting the mean LPF values and creating a bigger spread in the distribution. All joists exhibited higher mean LPF values than the nominal value models as shown in Table 4 and 5. This differences show a parallel behavior to the collected data since both HRS and CFS materials show higher mean yield strength values relative to nominal. Another important outcome of the sensitivity study is the differences between nominal LPF value and the mean LPF value are higher for Joist II than Joist I for the yield strength sensitivity analysis. This difference between the two joist types can also be explained by the collected data. The CFS material has a higher mean yield stress than HRS materials as it was shown in Table 3. Therefore, the CFS systems have a higher sensitivity to the yield strength value than HRS material systems and as a result the increase in the mean LPF values are higher

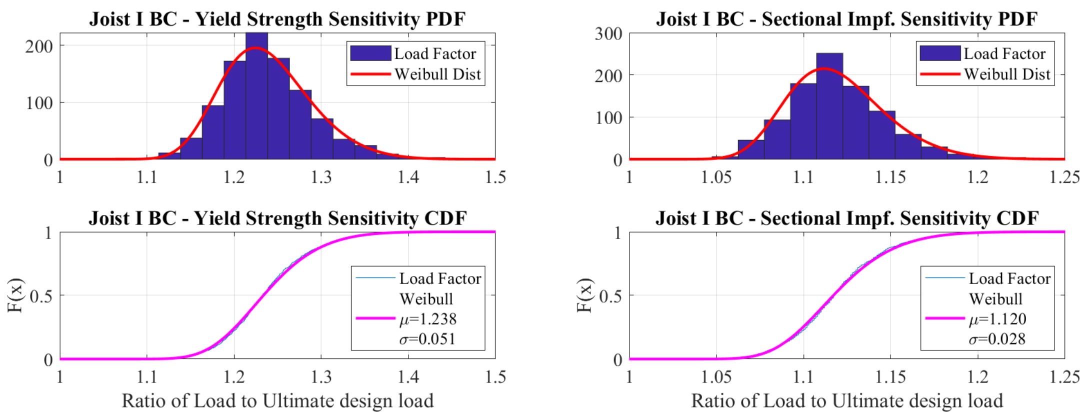

(a) Fitted distribution type for LPF results

(b) Fitted distribution type for LPF results

Figure 16: Joist I BC sensitivity analyses results and fitted distributions

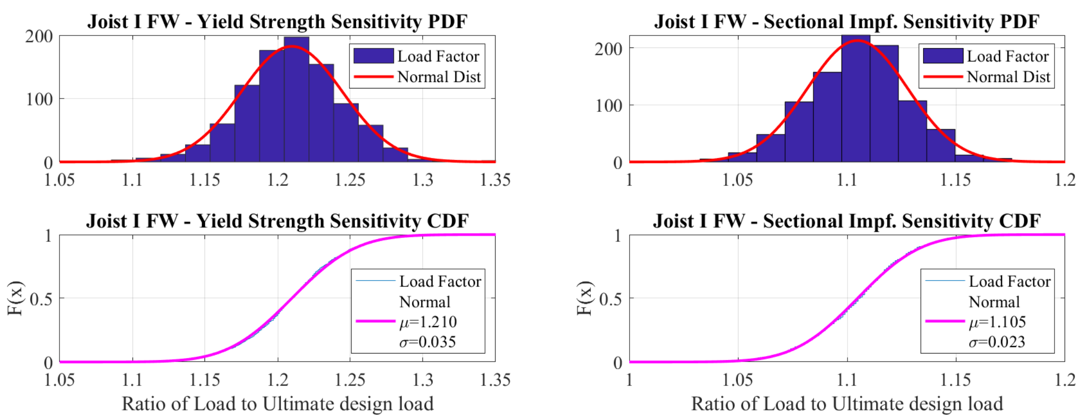

(a) Fitted distribution type for LPF results

(b) Fitted distribution type for LPF results

Figure 17: Joist I FW sensitivity analyses results and fitted distributions

5.4 Discussion

The first outcome of this study is that both beam and shell element FE models show that including the material nonlinearity and using the semi-rigid web end connections instead of pinned-end webs increases the overall load-carrying capacity of the joist designs. Additionally, the sensitivity analyses demonstrate that yield strength has the most significant influence on joist performance, particularly for CFS designs, where higher mean yield strength values resulted in greater increases

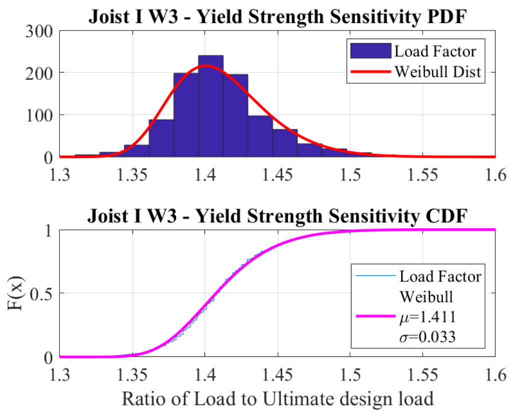

(a) Fitted distribution type for LPF results

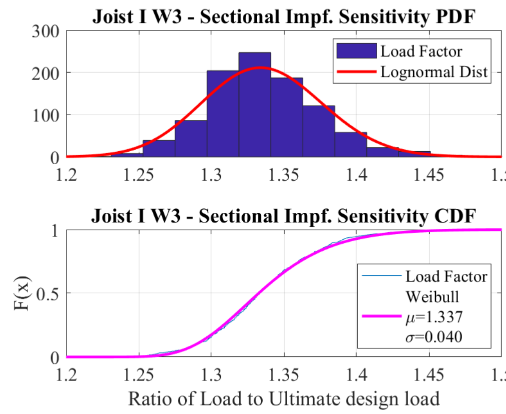

(b) Fitted distribution type for LPF results

Figure 18: Joist I W3 sensitivity analyses results and fitted distributions

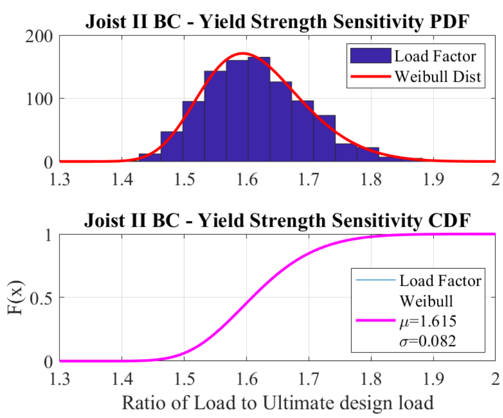

(a) Fitted distribution type for LPF results

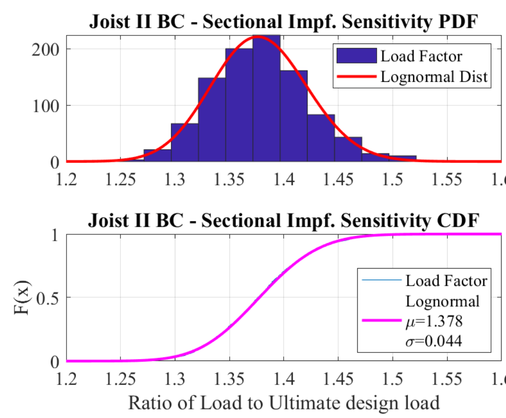

(b) Fitted distribution type for LPF results

Figure 19: Joist II BC sensitivity analyses results and fitted distributions

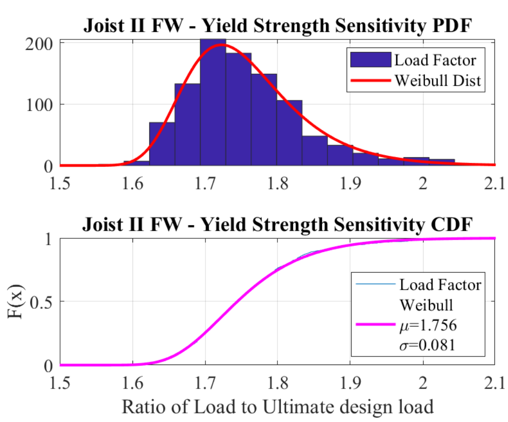

(a) Fitted distribution type for LPF results

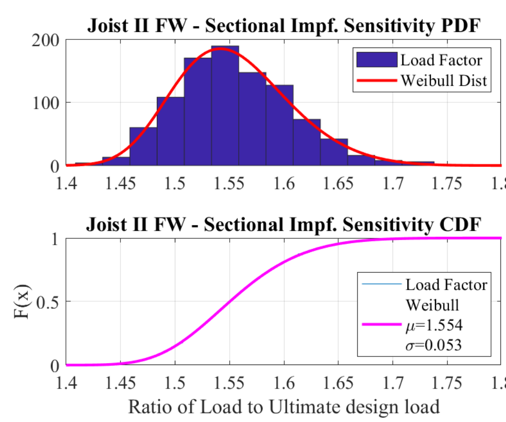

(b) Fitted distribution type for LPF results

Figure 20: Joist II FW sensitivity analyses results and fitted distributions

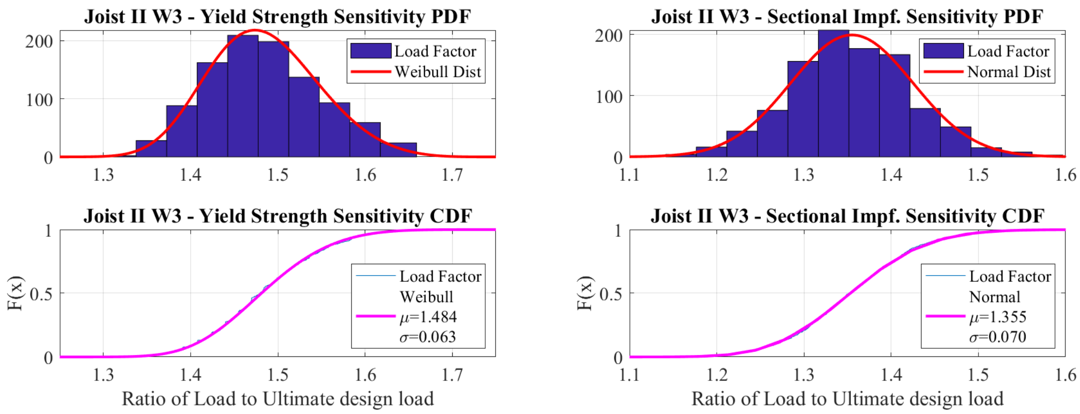

(a) Fitted distribution type for LPF results

(b) Fitted distribution type for LPF results

Figure 21: Joist II W3 sensitivity analyses results and fitted distributions

Table 4: Sensitivity analysis results

Failure Mode	**Distribution Type**	**Mean**	**Standard Deviation**
HRS BC Yield Strength	Weibull Dist.	1.238	0.051
HRS BC Sect. Impf.	Weibull Dist.	1.120	0.028
HRS FW Yield Strength	Normal Dist.	1.210	0.035
HRS FW Sect. Impf.	Normal Dist.	1.105	0.023
HRS W3 Yield Strength	Weibull Dist.	1.411	0.033
HRS W3 Sect. Impf.	Weibull Dist.	1.337	0.040
CFS BC Yield Strength	Weibull Dist.	1.615	0.082
CFS BC Sect. Impf.	Lognormal Dist.	1.378	0.044
CFS FW Yield Strength	Weibull Dist.	1.756	0.081
CFS FW Sect. Impf.	Weibull Dist.	1.554	0.053
CFS W3 Yield Strength	Weibull Dist.	1.484	0.063
CFS W3 Sect. Impf.	Normal Dist.	1.355	0.070

Modes: BC: bottom chord failure, FW: first web failure, W3: first web buckling failure

in LPF mean values compared to HRS designs, which can be explained by the collected data. Cross-sectional imperfections sensitivity showed that the changes in the cross-sectional properties caused reductions in joist capacity by up to 15% under specific conditions, emphasizing the need for quality control in manufacturing processes. Weld length variations, however, showed negligible impact on joist performance, indicating sufficient weld length in the data at hand. As a result, these findings highlight the importance of both material and geometric parameters in providing safe and efficient joist designs.

Table 5: Mean LPF values for sensitivity analysis results, and nominal model LPF values

		Sensitivity Analysis Mean LPF Results		
Model	**Nominal Model**	**Yield Stress**	**Sect. Impf.**	**Weld Length**
Joist I BC	1.109	1.238	1.120	1.110
Joist I FW	1.106	1.210	1.105	1.106
Joist I W3	1.323	1.411	1.337	1.325
Joist II BC	1.362	1.615	1.378	1.362
Joist II FW	1.560	1.756	1.554	1.529
Joist II W3	1.230	1.484	1.355	1.270

Modes: BC: bottom chord failure, FW: first web failure, W3: first web buckling failure

6. Conclusions

Sensitivity studies on open-web steel joists were conducted to determine the impact of the variability of modeling parameters including yield strength, cross-sectional dimensions, and weld length. Two joist designs with three expected failure modes each were investigated. A beam finite element model was used for the study, which was validated with a comprehensive shell finite element model. Data on yield strength, geometric variability of cross-sections, and weld length were collected from SJI member companies. The data was analyzed to determine best-fit distributions, and the sensitivity studies were conducted for each parameter of interest for each of the joist models, while all other variables were held at nominal values.

Overall, including any of the measured values of the input parameters provided an increase in strength compared to design predictions. It was found that yield strength had the most significant impact on joist strength compared to cross-sectional imperfections and weld length. Furthermore, the variability in weld length had a negligible impact on the joist performance with the data range under consideration. The results of this study contribute to the understanding of manufacturing tolerances and design assumptions on the capacities of open-web steel joists.

Acknowledgments

The authors would like to thank the Steel Joist Institute (SJI) for supporting the project through a research grant.

References

Abaqus (2016). *version 6.16*. Dassault Systèmes Simulia Corp.

AISC 360-16 (2016). *Specification for Structural Steel Buildings*. ANSI/AISC.

AISC 360-22 (2022). *Specification for Structural Steel Buildings*. ANSI/AISC.

American Iron and Steel Institute (2020). *S100-16 (R2020): North American Specification for the Design of Cold-formed Steel Structural Members*. Washington, DC, U.S.A.

Cicek, K., T. Sputo, and H.B. Blum (2024). "The impact of analysis assumptions on buckling prediction in open-web steel joists". *Proceedings of the Annual Stability Conference Structural Stability Research Council, SSRC 2024*.

Gardner, Leroy and Xiang Yun (2018). “Description of stress-strain curves for cold-formed steels”. *Construction and Building Materials* 189, pp. 527–538.

Kucukler, Merih, Leroy Gardner, and Lorenzo Macorini (2014). “A stiffness reduction method for the in-plane design of structural steel elements”. *Engineering Structures* 73, pp. 72–84.

Olsson, Anders MJ and Göran E Sandberg (2002). “Latin hypercube sampling for stochastic finite element analysis”. *Journal of Engineering Mechanics* 128.1, pp. 121–125.

Rasmussen, Kim JR, Xi Zhang, and Hao Zhang (2016). “Beam-element-based analysis of locally and/or distortionally buckled members: Theory”. *Thin-Walled Structures* 98, pp. 285–292.

Trahair, NS and GJ Hancock (2004). “Steel member strength by inelastic lateral buckling”. *Journal of structural Engineering* 130.1, pp. 64–69.

Yun, Xiang and Leroy Gardner (2017). “Stress-strain curves for hot-rolled steels”. *Journal of Constructional Steel Research* 133, pp. 36–46.

Zhang, Xi, Kim JR Rasmussen, and Hao Zhang (2015). “Beam-element-based analysis of locally and/or distortionally buckled members: Application”. *Thin-Walled Structures* 95, pp. 127–137.